

Tripling to 250 GHz with Planar Multiple Barrier Heterostructure Barrier Varactors

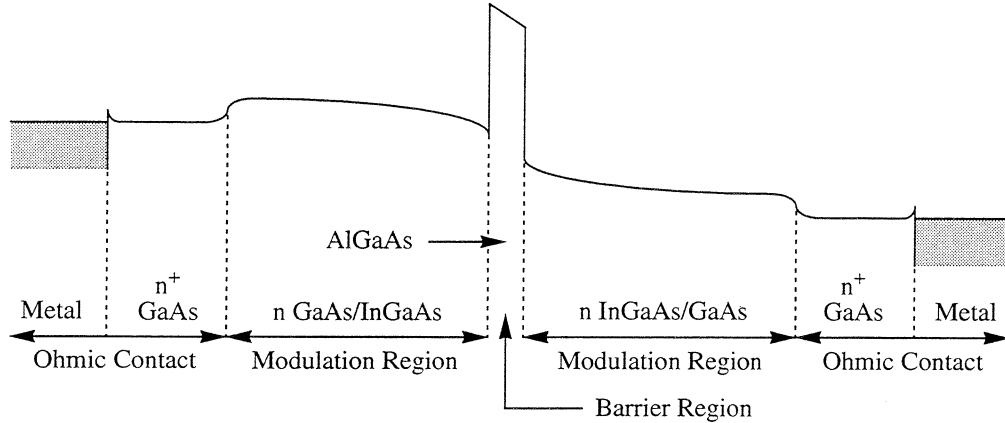
J.R. Jones, S.H. Jones, W.L. Bishop, R. Lipsey
Applied Electrophysics Laboratory, Department of Electrical Engineering
Charlottesville, Virginia 22903-2442
shj2n@virginia.edu
<http://fulton.seas.Virginia.EDU/~shj2n/sjrg>

We report on the design, simulation, fabrication, and testing of four-barrier, planar, heterostructure barrier varactor (HBV) triplers. For direct tripling, HBVs are an ideal device since the C-V characteristic is symmetric and only odd-harmonic generation occurs under large signal excitation. However, the optimal design of HBVs for specific applications is more complex than for conventional Schottky Barrier Devices. This is a direct result of the complex nature of the heterostructure, as well as the nearly infinite number of variations in heterostructure materials and the number of barriers to be considered. The fabrication process is similar to that used at the University of Virginia for the fabrication of multiple-anode Schottky Barrier Varactors. An overview of the fabrication process and the DC and RF testing results are discussed. Specific results demonstrating 2.5 mW of output power at 252 GHz (80 mW input) are reported for this direct tripler.

Introduction

The HBV¹, first proposed in 1989 [1], has received considerable attention [2-10] as a promising device for high efficiency frequency multiplication in the millimeter to submillimeter wavelength range because of its attractive device characteristics and large number of design parameters. A single barrier HBV consists of a large bandgap semiconductor sandwiched between symmetric moderately doped modulation regions of smaller bandgap material (see Figure 1) such that the device has an evenly symmetric nonlinear capacitance-voltage (C-V) relationship about zero d.c. bias. This evenly symmetric device C-V characteristic eliminates the even-harmonic components from the output current waveform so that high efficiency frequency multiplier circuits, which do not require d.c. bias and which require fewer idlers than standard Schottky Barrier Varactor (SBV) multipliers, can be realized. These device characteristics make the HBV an ideal device for use in high order frequency multipliers, broadband frequency multipliers, and quasi-optical tripler arrays. The HBV is ideally suited for use as the multiplier element in a quasi-optical

1. Although this device was originally called the Quantum Barrier Varactor (QBV) and is often called the Single Barrier Varactor (SBV), it is called the Heterostructure Barrier Varactor (HBV) throughout this work to avoid confusion with the Schottky Barrier Varactor (SBV) and to emphasize the importance of the heterostructure alloy composition and doping profiles in the design and operation of the device.



1. One-dimensional schematic diagram, in an illustrative material system, of a Heterostructure Barrier Varactor showing ohmic contact, modulation, and barrier regions.

tripler array since no idlers are required for frequency tripling and d.c. bias is not required for the individual elements in the array.

By epitaxially stacking several single barrier HBVs in series, further advantages are obtained including increased device impedances for a given device area, higher device cut-off frequencies for a given device area due to reduced device capacitances, higher power handling capabilities due to the distribution of pump power over several series devices, and increased heat dissipation capabilities for a given capacitance modulation range due to increased device areas. Overall, the HBV has a large degree of design flexibility in that the semiconductor alloy composition and doping profiles, barrier thickness, number of barriers, device geometry, and device area can all be varied. Ultimately, the design flexibility and attractive device characteristics of the HBV suggest that a high efficiency frequency multiplier with excellent device/circuit impedance matching and near-optimum C-V relationship can be achieved with a single device.

In this paper we describe the first time fabrication and testing of planar and multiple barrier HBVs. A total of four GaAs/AlGaAs heterostructure barriers have been used in this device. The epitaxial material is grown on a semi-insulating GaAs substrate and includes an n+ buffer, two GaAs/AlGaAs barrier regions, and three GaAs modulation regions. After fabrication of the monolithic device there are two surface channel ohmic contact structures and a total of four

barriers; two barriers are under one contact and two are under the other contact connected by the underlying n^+ buffer region. The device has been designed using the previously described numerical simulation technique [11], and the device fabrication process is similar to that used to fabricate University of Virginia planar Schottky Barrier Varactors [12,13]. This planar HBV has been designed to have the same terminal characteristics as the commonly used UVa 6P4 Schottky Barrier Varactor [14] in order to better guarantee successful operation of this novel device.

Device Fabrication

Heterostructure Barrier Varactor (HBV) devices were fabricated for d.c., microwave, and millimeter wave testing purposes. Planar multi-barrier HBV devices for tripling from 80 GHz to 240 GHz were fabricated using a process in which the device "surface channel" is etched prior to formation of the contact pad-to-anode air-bridge "finger" [15,16]. The formation of the device air-bridge "finger" after the "surface channel" etch is facilitated by a trench planarization technique, and yields a device with minimum parasitic capacitances.

All of the HBV material structures utilized in this work were provided by the Naval Research Laboratories (NRL). The structures were grown in a Vacuum Generators V80H Molecular Beam Epitaxy (MBE) system on (100)-oriented GaAs substrates manufactured by American Xtal Technology. Planar multi-barrier HBV structures were grown on semi-insulating (SI) substrates with resistivities of $5.0\text{-}7.0 \times 10^7 \Omega\text{-cm}$ at 300 K. Alloy composition and silicon doping profiles as well as layer thicknesses for the NRL-grown structures were estimated based on values extracted from calibration structures grown in the MBE system. The MBE-grown epitaxial structure for the prototype HBVs is given Table 1 shown below.

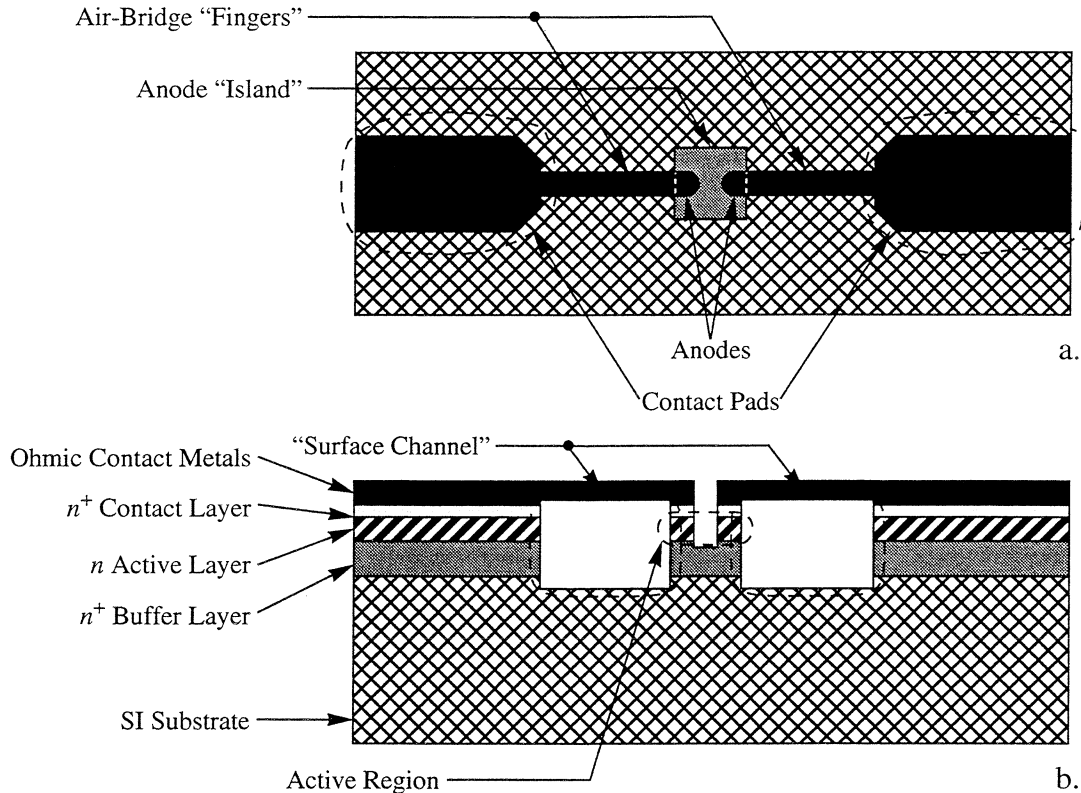
Ohmic contacts were formed by alloying the anode and cathode Au(650 Å)/Ge(325 Å)/Ni(250 Å)/Ti(400 Å)/Au(2000 Å) metallization structures for 2 minutes in an alloy furnace purged with forming gas (90% N_2 /10% H_2). As shown in Table 1 the planar HBV structures have an n^+ InAs/ $\text{In}_{1.0-0.0}\text{Ga}_{0.0-1.0}\text{As}$ /GaAs epitaxial capping layer at the surface for forming very low resistance ohmic contacts [17]. The alloy temperature was approximately 375 °C, and the contact morphology was excellent and unchanged after alloy. TLM test structures consisting of 100 μm wide by 150 μm long contact pads were fabricated on the two different HBV epitaxial structures (one having an n^+ GaAs capping layer and one having an n^+ InAs/ $\text{In}_{1.0-0.0}\text{Ga}_{0.0-1.0}\text{As}$ /GaAs

capping layer) to determine the resistance of the ohmic contacts. Average specific contact resistivities for the structures with n^+ GaAs (400 °C) and n^+ InAs/In_{1.0-0.0}Ga_{0.0-1.0}As/GaAs (375 °C) capping layers were approximately $2.14 \times 10^{-6} \Omega \cdot \text{cm}^2$ and $6.82 \times 10^{-7} \Omega \cdot \text{cm}^2$, respectively.

	Layer Thickness	Layer Doping	Material
n⁺ Contact Layer	100 Å	n^+	InAs
	400 Å	n^+	In _{1.0-0.0} Ga _{0.0-1.0} As
	3000 Å	n^+	GaAs
n Active Layer	2500 Å	$n (8 \times 10^{16} \text{ cm}^{-3})$	GaAs
	35 Å	i	GaAs
	200 Å	i	Al _{0.7} Ga _{0.3} As
	35 Å	i	GaAs
	5000 Å	$n (8 \times 10^{16} \text{ cm}^{-3})$	GaAs
	35 Å	i	GaAs
	200 Å	i	Al _{0.7} Ga _{0.3} As
	35 Å	i	GaAs
	2500 Å	$n (8 \times 10^{16} \text{ cm}^{-3})$	GaAs
n⁺ Buffer Layer	4 μm	n^+	GaAs
Substrate	450 μm	SI	GaAs

Table 1 Epitaxial material structure for the 4 barrier, planar HBVs.

Unlike the Schottky Barrier Varactor (SBV) where the cross-sectional area controlling charge modulation is defined by the area of the anode, the cross-sectional area controlling charge modulation in an HBV is defined by the cross-sectional areas of both the barrier and modulation regions of the device. As a result, the fabrication of planar HBVs requires either an ion implant isolation step or a mesa-isolation etch step to define the active region of the device. In the present work, planar mesa-isolated HBVs have been produced using a fabrication procedure in which the device “surface channel” is etched prior to formation of the contact pad-to-anode air-bridge



2. Top (a.) and cross-sectional (b.) views of the planar HBV device layout.

“finger”. Formation of the device air-bridge “finger” after etching the “surface channel” is facilitated by using the trench planarization technique of reference [15-16], and yields a device with minimal parasitic capacitances since the fringing capacitances between the device active region “mesa” and the air-bridge “finger” are minimized.

The basic planar HBV device layout used in this work is shown below. This back-to-back layout yields an inherently multi-barrier device; it has been utilized here to compensate for any asymmetry in the MBE-grown epitaxial structure and to double the number of barriers obtained from a given HBV epitaxial structure. The general planar HBV fabrication process developed for this work is outlined schematically in Figure 3. An overview of this process is given, in reference to Figure 3, below:

- a. Deposit Au(650 Å)/Ge(325 Å)/Ni(250 Å)/Ti(400 Å)/Au(2000 Å) ohmic contact metallization in device anode and contact pad regions using a dual-layer

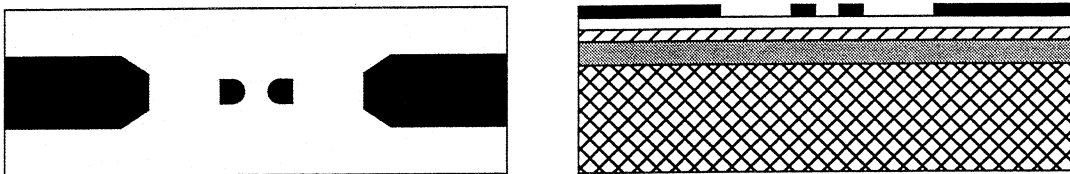
photoresist/electron-beam evaporation lift-off process, and alloy ohmic contacts in a forming gas ambient (90% N₂/10% H₂) for 2 minutes.

- b. Form device "surface channel" to isolate anode and contact pad regions using a photoresist protection/reactive-ion etch process.
- c. Planarize device "surface channel" using a low viscosity thermosetting epoxy and a planarizing superstrate. The bulk epoxy planarization process used here was developed by W. Bishop at UVa.
- d. After exposing the device contact pads and anodes by O₂ plasma etching the epoxy, spin a very thin layer of photoresist on the wafer to improve the uniformity of the bulk epoxy planarization step, and redefine the device contact pads and anodes in the photoresist.
- e. Sputter deposit Cr/Au "seed" metallization on entire wafer, pattern contact pad-to-anode air-bridge "finger" structures in photoresist, and d.c. electroplate the entire contact pad/air-bridge "finger"/anode structures.
- f. Remove epoxy/photoresist planarization material using an O₂ plasma etch process
- g. Isolate device anodes using a photoresist protection/reactive-ion etch process.

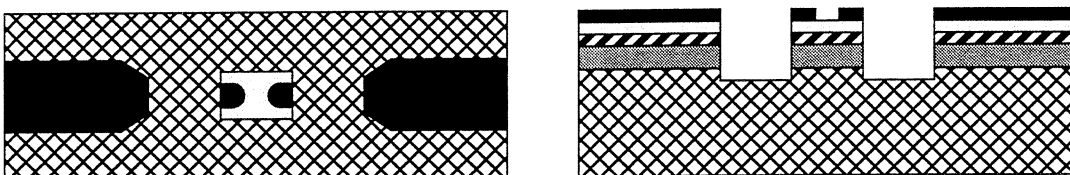
The fabrication process is completed by making dice cuts at the boundaries of the individual chips while protecting the frontside of the wafer with a polymer protective coating, and lapping the backside of the wafer in order to thin the wafer and separate the individual chips.

A given photolithographic level on the mask used to fabricate these devices contained of an array of devices with 6 μm (3 μm), 8 μm (3 μm, 4 μm, and 5 μm), and 10 μm (4 μm) anode diameters ("finger" widths). For all devices, the contact pads were 30 μm wide and 60 μm long, while the "fingers" were 50 μm long and the anodes were spaced 5 μm apart. Figure 4 shows a scanning electron micrograph of a completed prototype four barrier GaAs/Al_{0.7}Ga_{0.3}As HBV having 8 μm diameter anodes, 4 μm wide "fingers", and a total chip thickness of approximately 2.25 mils. The etch depth for the device "surface channel" is approximately 10 μm, while the height of the anode "mesas" is approximately 3 μm. The actual anode diameter is approximately 8.75 μm since a 1.5 minute 10:1 50 % citric acid:H₂O₂ wet chemical etch was used to improve the quality of the "mesa" sidewalls and the anode isolation region following the device anode reactive-ion isolation etch

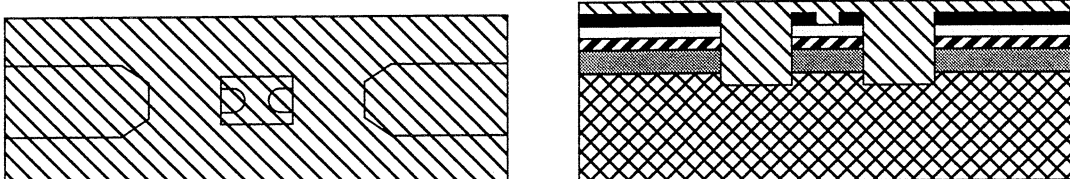
a. Metallization of device anode and contact pad ohmic contacts



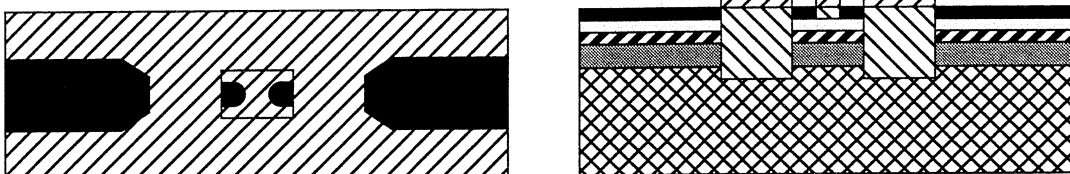
b. Reactive-ion etch of device "surface channel"



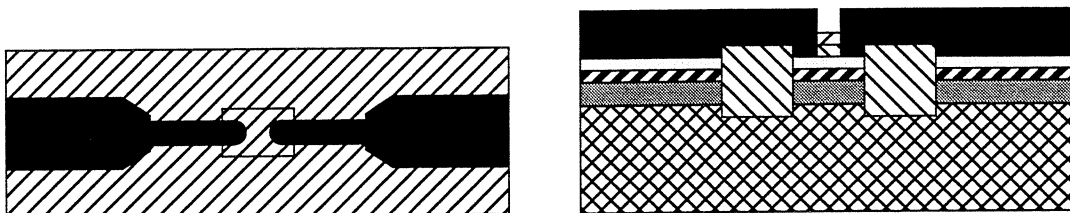
c. Bulk (epoxy) planarization of device "surface channel"



d. Final (photoresist) planarization of device "surface channel"

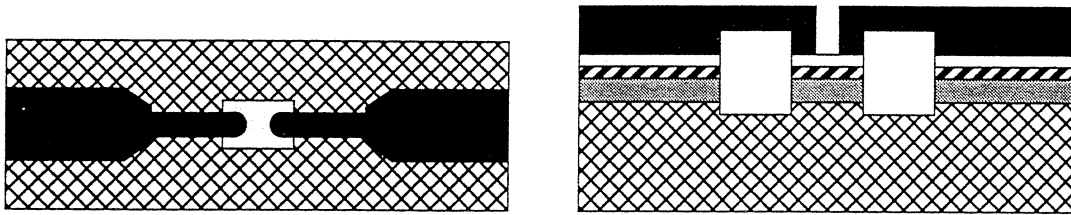


e. Electroplating of Au device air-bridge "fingers"

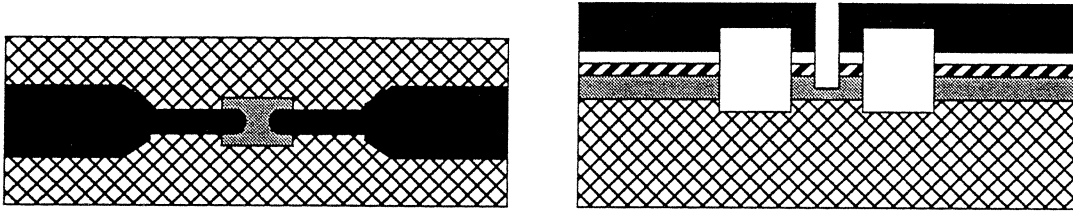


3. Top and cross-sectional views of the fabrication steps for the fabrication of planar HBVs.

f. Removal of epoxy/photoresist planarization material



g. Reactive-ion etch to isolate device anodes



Legend:

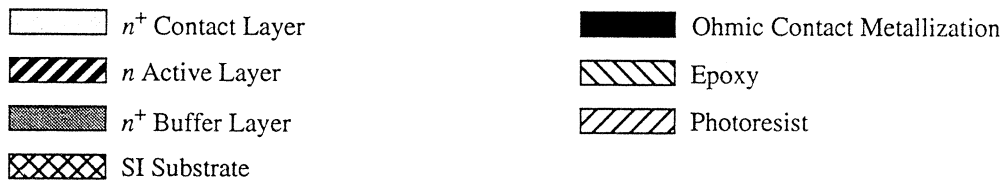
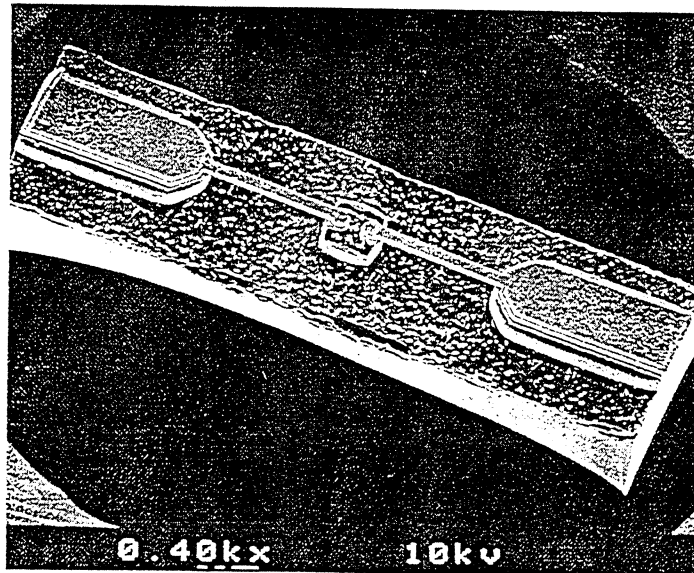


Figure 3 continued.

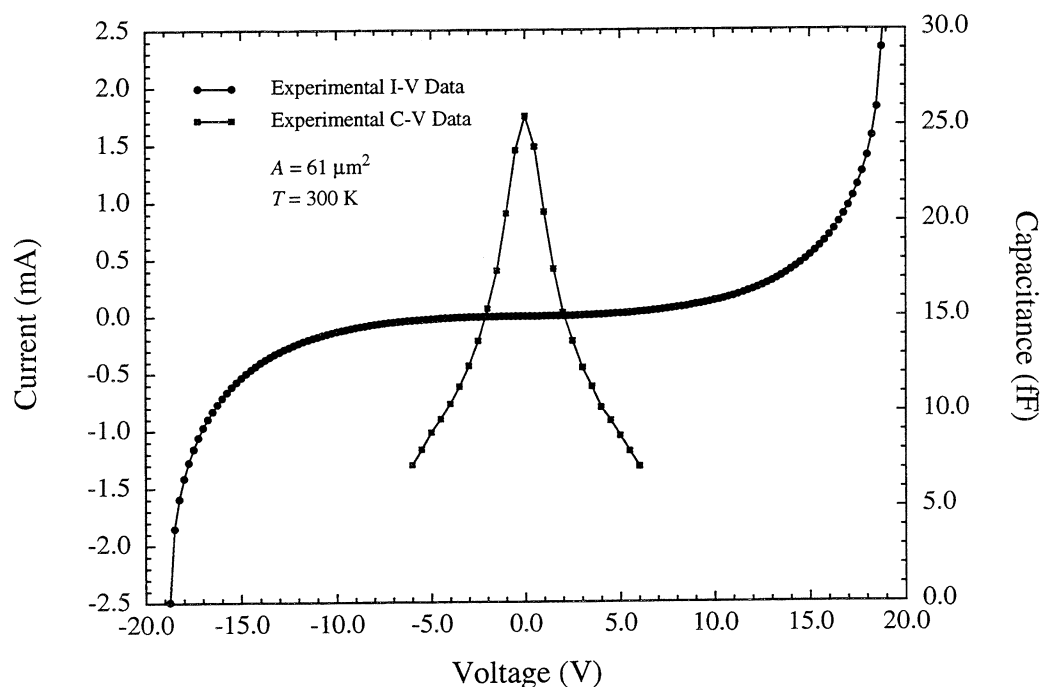


4. Scanning Electron Micrograph of fabricated planar HBV

DC and RF Testing

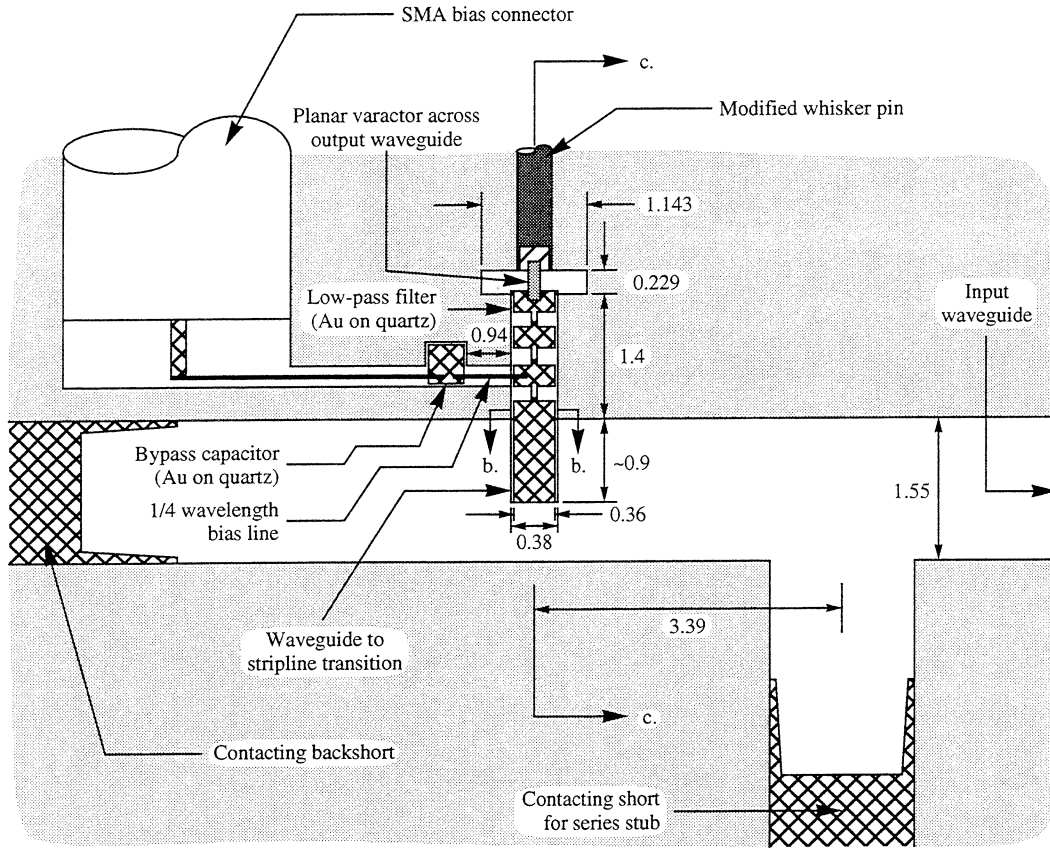
The planar four barrier GaAs/Al_{0.7}Ga_{0.3}As Heterostructure Barrier Varactor (HBV) devices were analyzed to determine their d.c. current-voltage (I-V) and static capacitance-voltage (C-V) characteristics. The d.c. I-V characteristics were measured using a Hewlett-Packard (HP) 4145B semiconductor parameter analyzer. The static C-V characteristics were measured using an HP 4275A multi-frequency LCR meter with a local oscillator voltage between 0.01 V and 0.04 V, and an excitation frequency of 4 MHz; the devices were biased using a Keithley 238 high current source measure unit.

Figure 5 shows the experimental d.c. I-V and static C-V characteristics of the UVA-NRL-1174-K planar four barrier GaAs/Al_{0.7}Ga_{0.3}As HBVs with nominal 10 μm diameter anodes; a series impedance of 4.9 Ω has been estimated for these devices.

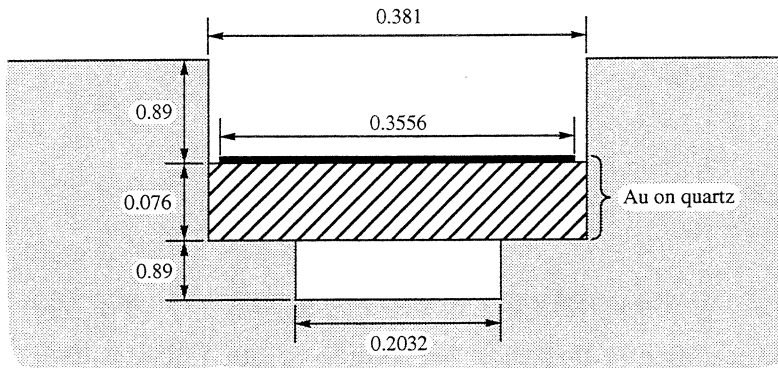


5. Experimental DC current-voltage, and capacitance-voltage planar HBV characteristics

Figure 6 is a detailed schematic diagram of the internal configuration of the tripler block utilized here. Input power is coupled to the device under test via a waveguide probe (waveguide to stripline transition) which extends into the WR-12 input waveguide. A stripline filter is integrated onto the waveguide probe to prevent power at harmonics above the fundamental from reaching the



a.



b.

6. Schematic diagrams of the NRAO A2621-TR2-T12 200-290 GHz tripler block showing (a.) the block split along the partition between the block halves, (b.) a cross-section of the stripline filter channel, (c.) a cross-section through the block detailing the output waveguide transformer and device under test mounting configuration, and (d.) the configuration for the output backshort. Note that all dimensions are in millimeters.

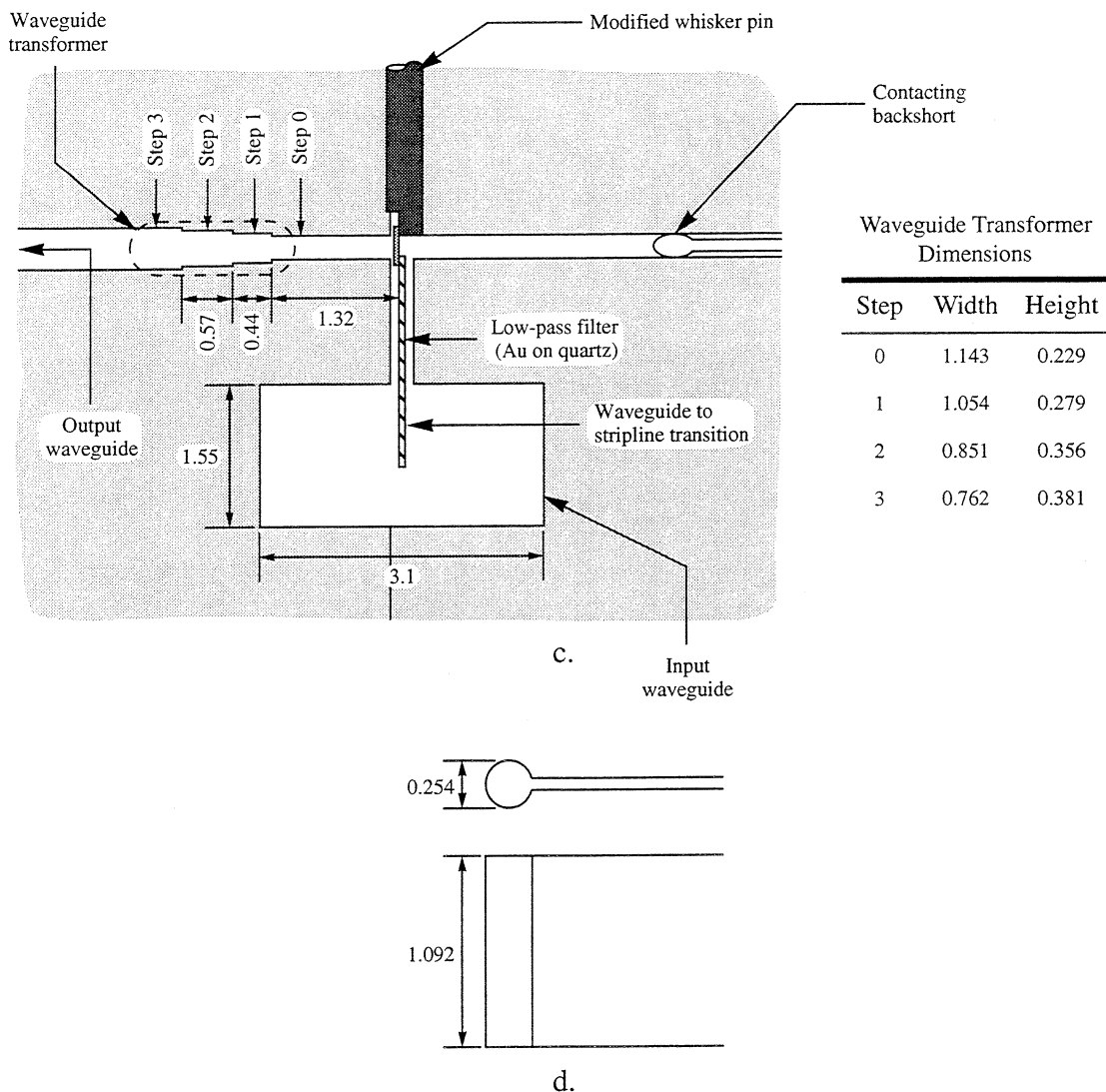


Figure 6 continued.

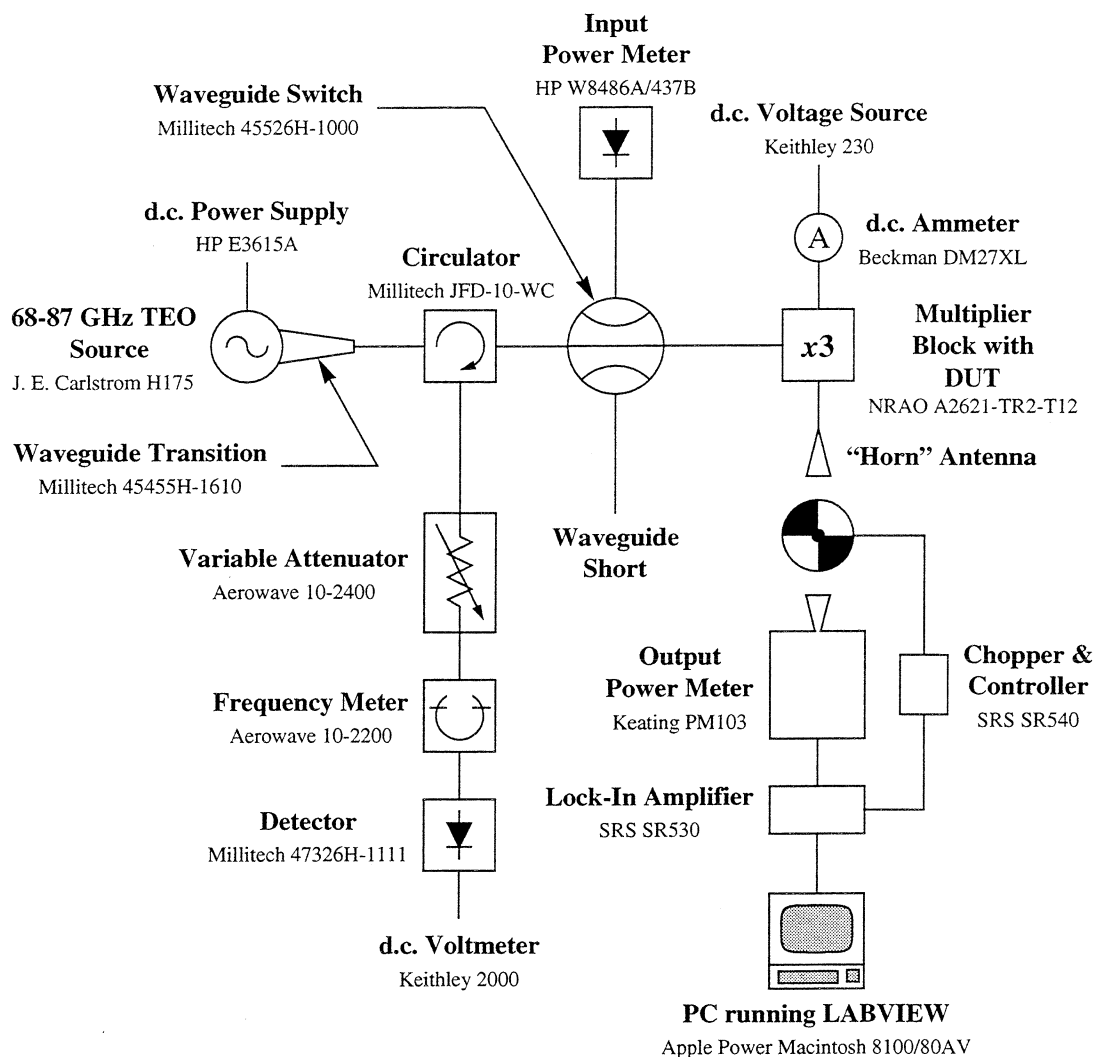
input waveguide. Near the device under test, a two-section quarter-wave impedance transformer is used to couple the reduced-height backshort waveguide to the WR-3 output waveguide. The transformer, spaced approximately a half wavelength from the plane of the device under test, acts as a reactive idler at the second harmonic frequency. The output waveguide is cut-off at both the fundamental and second harmonic frequencies. The block is equipped with three separate adjustable contacting short-circuit tuners, a backshort tuner and an E-plane tuner on the input waveguide as well as a backshort tuner on the output waveguide. It is important to note that the output waveguide backshort is utilized to tune both the output circuit at the third-harmonic

frequency and the idler circuit at the second harmonic frequency. Finally, d.c. bias to the device under test is provided via a $140\ \Omega$ transmission line bias filter. The transmission line consists of a 1 mil diameter Au wire which is bonded between one of the low-impedance sections of the stripline filter and a 100 fF Au on quartz dielectric capacitor. The capacitor is enclosed in a rectangular shield machined into the block, and acts as an r.f. short-circuit which is transformed to an open-circuit at the stripline filter.

An array of waveguide probe/stripline filter structures (ATR1) were fabricated for this work on 3 mil thick quartz using standard optical photolithography, metallization, and sputter etching procedures. First, a $50\ \text{\AA}/2000\ \text{\AA}$ Cr/Au "seed" layer was sputter deposited on the quartz substrate. After defining the array of stripline filter structures in photoresist, the Au filter structures were d.c. electroplated to a thickness of approximately $2.5\ \mu\text{m}$. After removing the photoresist, the exposed "seed" metallization was removed via an Ar sputter etch process. Finally, the substrate was diced to separate the individual circuits.

In order to support planar devices across the output waveguide, the whisker pin of the block was modified. This minor modification, which was performed by R. F. Bradley and N. Horner at NRAO, involved milling out a flat surface on the side of the whisker pin such that the milled out surface was in the plane of the top side of the stripline filter circuit. Ideally, the distance between the plane of this flat surface and the upper half of the block is approximately 3.5 mils. As such, the planar HBVs were lapped to a thickness of about 2.25 mils to accommodate the combined heights of the epoxy used to secure the stripline circuit, the device, and the solder used to secure the device.

After wire bonding a long 1 mil Au wire to the last stripline filter circuit low impedance section and trimming the length of this Au wire to approximately 1.25 mm, the circuit was secured in the tripler block using a 90 minute curing epoxy. The free end of the Au wire was then wire bonded to the Au on quartz dielectric capacitor to complete the bias circuit. Finally, to accommodate device mounting, indium bumps were formed on the end of the stripline filter circuit and on the flat surface of the whisker pin using pure indium and SuperSafe Flux No. 3, and heating the block to approximately $160\ ^\circ\text{C}$ until the indium melted. Planar HBVs were mounted across the output waveguide by pressing the devices into the indium bumps without heating the block. Since the planar HBVs were approximately 11.75 mils long and the stripline filter circuit extended into



7. Test setup for measuring the performance of frequency multipliers.

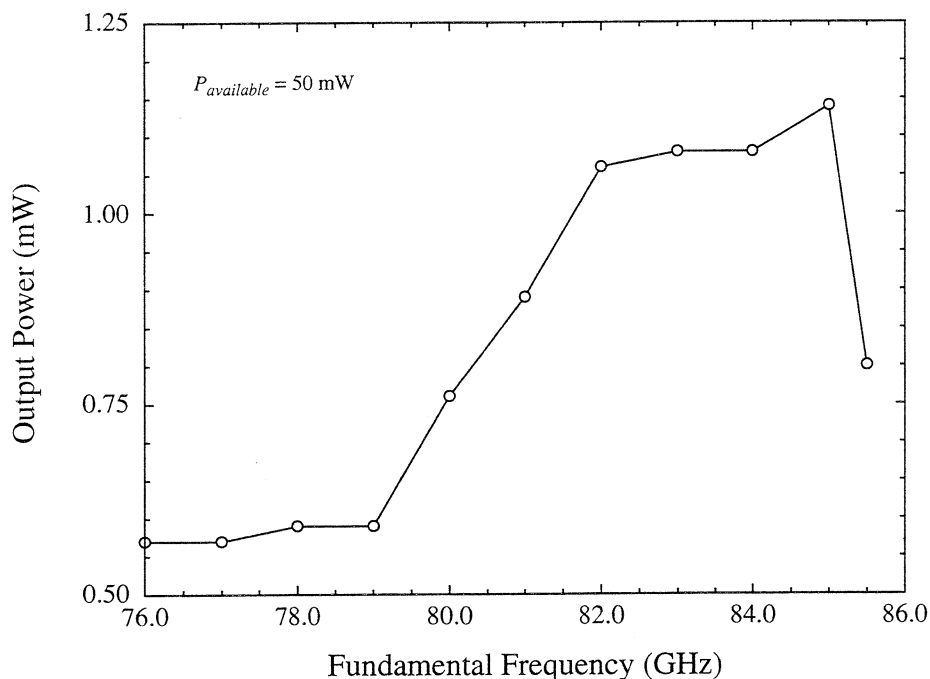
the output waveguide by about 2 mils (the whisker pin did not extend into the output waveguide), there was about 4.75 mils of overlap for mounting the devices.

The performance of planar HBV triplers was evaluated using three types of measurements: (1) output power versus frequency with 50 mW of input power, (2) output power versus input power at the frequency of highest tripling efficiency, and (3) input return loss versus frequency with 50 mW of input power. Except for output power versus input power measurements above 60 mW of input power, the test setup of Figure 7 was utilized for all measurements. Due to excessive losses in the circulator, waveguide switch, and sections of waveguide between the input

power source and the tripler block, the source was connected directly to the tripler block for output power versus input power measurements above 60 mW of input power.

The input power source for the measurement test setup is a mechanically tuned, low noise Transferred Electron Oscillator (TEO) which produces up to 100 mW of power at frequencies from 68 GHz to 87 GHz [18]. The amount of input power supplied to the multiplier block is controlled by an adjustable output waveguide backshort on the TEO cavity; the frequency of oscillation is controlled by an adjustable "top-hat" on the cavity. The input power is measured using a Hewlett-Packard W8486A power sensor operating, from 75 GHz to 110 GHz, with a dynamic range of -30 dBm to 20 dBm. Finally, the output power from the tripler block is measured using a PM103 Terahertz Absolute Power Meter System manufactured by Thomas Keating, Ltd. The output power meter operates from 30 GHz to 3 THz, and employs a closed, air-filled cell detector to measure the power contained in incident free-space beams. The closed cell detector contains a metal film which absorbs a known fraction of the power incident on the cell. The incident beam is amplitude modulated by a chopper at a frequency of approximately 27 Hz such that the absorption of power in the metal film produces modulated variations in the temperature of the film. This, in turn, produces a modulation of the pressure in the cell which is detected by a pressure transducer. The output voltage from the pressure transducer is measured by a lock-in amplifier and represents the sensitivity of the power meter to the incident power. The meter is calibrated by generating a known amount of ohmic power in the metal film; the ohmic power is generated by passing a modulated current through the film at the same modulation frequency as that used to modulate the input beam. Manufacturer-supplied calibration factors account for loss in the meter's input "window" as a function of frequency, fractional film absorption, and fractional cell transmission. In order to eliminate reflections from the input "window", the meter is set so that the incident beam is oriented at the Brewster angle (55°) with the plane of polarization in the plane of incidence.

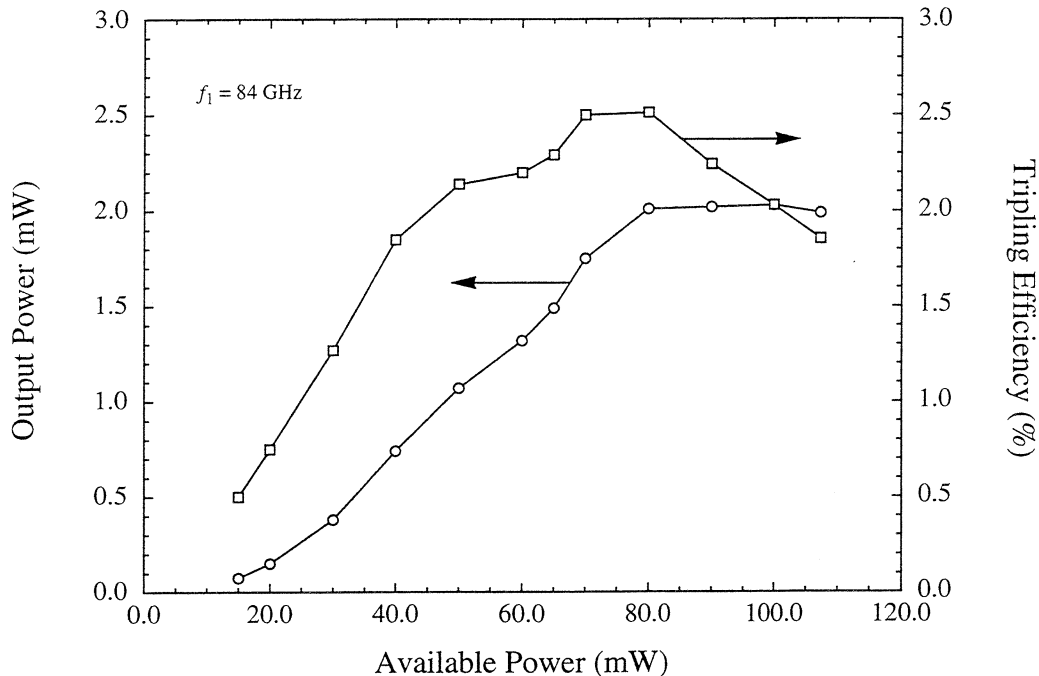
In order to accurately measure absolute power, it is important to ensure that all of the detected power comes from the incident beam. Since the Keating absolute power meter is broadband, any modulated power from external thermal, optical, or acoustic sources will be detected. These "noise" sources were minimized by (1) minimizing the distances between the tripler output "horn" antenna, the chopper blade, and the detector, and (2) placing a sheet of



8. Output power versus fundamental frequency for the prototype planar four barrier GaAs/Al_{0.7}Ga_{0.3}As HBV triplers (UVA-NRL-1174-K) of Chapter 6 at an available power of 50 mW.

absorptive material directly behind the chopper blade with only the tripler “horn” antenna passing through the sheet as necessary.

The performance of the prototype planar four barrier GaAs/Al_{0.7}Ga_{0.3}As HBV triplers was evaluated near the 80/240 GHz center frequency of the NRAO tripler block described above. Devices with nominal anode diameters of 10 μm (approximately 8.75 μm after wet etching) were tested. For an input (available) power of 50 mW, the output power versus fundamental frequency for frequencies between 76 GHz and 85.5 GHz is shown in Figure 8. More than 1 mW of power was generated at fundamental frequencies between approximately 81.5 GHz and 85.25 GHz. The input return loss for these measurements was better than -10 dB for fundamental frequencies between about 71.5 GHz and 85 GHz. At a fundamental frequency of 84 GHz, the output power versus available power is shown in Figure 9. A maximum output power of greater than 2 mW was generated at 252 GHz with an available power of 80 mW, yielding a peak flange-to-flange tripling efficiency of greater than 2.5 %. The device d.c. rectified current was 1-45 uA for powers ranging from 20-100 mW respectively. This indicates that the symmetry in the UVA-NRL-1174 material and device structures is quite good since the device d.c. rectified current is fairly low. For historical



9. Output power versus available power for the prototype planar four barrier GaAs/ $\text{Al}_{0.7}\text{Ga}_{0.3}\text{As}$ HBV triplers (UVA-NRL-1174-K) of Chapter 6 at a fundamental (output) frequency of 84 GHz (252 GHz).

comparison purposes, the initial whisker-contacted single barrier HBVs of reference [2] had a maximum output power (tripling efficiency) of approximately 1.25 mW (5 %) at an output frequency of 228 GHz (225 GHz). At an output frequency of 252 GHz, the maximum output power was only 1 mW with a tripling efficiency of only 3 %. Subsequent tests using these same whisker-contacted single barrier HBVs in a second tripler block yielded a maximum output power (tripling efficiency) of only about 0.8 mW (2 %) at an output frequency of 192 GHz. [6].

Conclusion

We have demonstrated that multiple-barrier planar HBVs can be fabricated using a novel fabrication process to etch the surface channel regions prior to the formation of the ohmic contact fingers. InAs ohmic contact structures have been used to reduce the contact resistance of both the cathode and the anode. DC and RF testing have been completed, and at least 2.5 mW of output power at 252 GHz has been achieved. These power and efficiency levels are expected to improve as the tripler circuit is improved and modified for HBVs. Also, the device design should be changed to shorten the length of the modulation regions which is expected to further improve device performance.

Acknowledgments

J.R. Jones has been supported by a United States Air Force Laboratory Graduate Fellowship under the sponsorship of the Solid-State Directorate, Wright Laboratory, WPAFB, OH. This research has been partially supported by NSF Grant ECS-9412931. The authors thank Erik Kollberg, Neal Erickson, and Tom Crowe for many helpful discussions.

References

1. E. Kollberg and A. Rydberg, "Quantum-Barrier-Varactor Diodes for High-Efficiency Millimeter-Wave Multipliers," *Electron. Lett.*, Vol. 25, No. 25, December 1989, pp. 1696-1698.
2. A. Rydberg, H. Grönqvist, and E. Kollberg, "Millimeter- and Submillimeter-Wave Multipliers Using Quantum-Barrier-Varactor (QBV) Diodes," *IEEE Electron Dev. Lett.*, Vol. 11, No. 9, September 1990, pp. 373-375.
3. H. Grönqvist, E. Kollberg, and A. Rydberg, "Quantum-Well and Quantum-Barrier Diodes for Generating Submillimeter Wave Power," *Microwave Optical Technol. Lett.*, Vol. 4, No. 1, January 1991, pp. 33-38.
4. H-X. L. King, L. B. Sjogren, N. C. Luhmann, Jr., and D. B. Rutledge, "New Concepts for High Frequency and High Power Frequency Multipliers and Their Impact on Quasi-Optical Monolithic Array Design," *Int. J. Infrared Millimeter Waves*, Vol. 13, No. 2, February 1992, pp. 251-266.
5. S. M. Nilsen, H. Grönqvist, H. Hjelmgren, A. Rydberg, and E. L. Kollberg, "Single Barrier Varactors for Submillimeter Wave Power Generation," *IEEE Trans. Microwave Theory Tech.*, Vol. 41, No. 4, April 1993, pp. 572-580.
6. D. Choudhury, M. A. Frerking, and P. D. Batelaan, "A 200 GHz Tripler Using a Single Barrier Varactor," *IEEE Trans. Microwave Theory Tech.*, Vol. 41, No. 4, April 1993, pp. 595-599.
7. H-X. L. Liu, L. B. Sjogren, C. W. Domier, N. C. Luhmann, Jr., D. L. Sivco, and A. Y. Cho, "Monolithic Quasi-Optical Frequency Tripler Array with 5-W Output Power at 99 GHz," *IEEE Electron Dev. Lett.*, Vol. 14, No. 7, July 1993, pp. 329-331.
8. K. Krishnamurthi, S. M. Nilsen, and R. G. Harrison, "GaAs Single-Barrier Varactors for Millimeter-Wave Triplers: Guidelines for Enhanced Performance," *IEEE Trans. Microwave Theory Tech.*, Vol. 42, No. 12, December 1994, pp. 2512-2516.
9. A. V. Räisänen, T. J. Tolmunen, M. Natzic, M. A. Frerking, E. Brown, H. Grönqvist, and S. M. Nilsen, "A Single Barrier Varactor Quintupler at 170 GHz," *IEEE Trans. Microwave Theory Tech.*, Vol. 43, No. 3, March 1995, pp. 685-688.
10. Numerous papers have also been published on HBVs in various conference proceedings, the most notable being the recent proceedings of the Int. Symp. on Space Terahertz Technol., the Int. Conf. on Infrared and Millimeter Waves, and the IEEE MTT-S Int. Microwave Symposium.
11. M.F. Zybura, J.R. Jones, S. H. Jones, G. Tait, "Simulation of 100-300 GHz Solid-State Harmonic Sources", *IEEE Trans. Microwave Theory and Tech.*, vol. 43, no. 4, April (1995), pp 955-961.
12. W. L. Bishop, K. McKinney, R. J. Mattauch, T. W. Crowe, and G. Green, "A Novel Whiskerless Schottky Diode for Millimeter and Submillimeter Wave Applications," *IEEE MTT-S Int.*

Microwave Symp. Dig., Las Vegas, Nevada, June 9-11, 1987, pp. 607-610.

13. W. L. Bishop, K. A. McLeod, and R. J. Mattauch, "Whiskerless Schottky Diode," U. S. Patent 5,041,881, August 20, 1991.

14. T.W. Crowe, W. Peatman, R. Zimmermann, R. Zimmermann, "Considerations of Velocity Saturation in the Design of GaAs Varactor Diodes", IEEE Microwave and Guided Wave Letters, vol. 3, no. 6, June (1993).

15. W. L. Bishop, T. W. Crowe, and R. J. Mattauch, "Planar GaAs Schottky Diode Fabrication: Progress and Challenges," Proc. Fourth Int. Symp. Space Terahertz Technol., March 30-April 1, 1993, Los Angeles, California, pp. 415-429.

16. W. L. Bishop, "Planar GaAs Mixer Diode Research," University of Virginia Semiconductor Device Laboratory Quarterly Report on Millimeter and Submillimeter Wave Receiver Element Research, January 1, 1995- September 30, 1995, p. 6.

17. N. Papanicolaou, S. H. Jones, J. R. Jones, W. T. Anderson, and R. S. Sillmon, "High Temperature Characteristics of Amorphous TiWSi(x) Non-Alloyed Ohmic Contacts to GaAs," J. Appl. Phys., Vol. 72, No. 10, November 1992, pp. 4954- 4957.

18. for example contact J.E. Carlstrom Co., Chicago, Ill., or see J.E. Carlstrom, R.L. Plambeck, D.D. Thornton, IEEE Trans. Microwave Theory and Tech., MTT-33, 610, (1985).